

# Chemical Engineering Journal

## Boosting heavy metals removal from water by reusable cryo-sponges based on N-methyl-D-glucamine --Manuscript Draft--

<b>Manuscript Number:</b>	CEJ-D-20-06112
<b>Article Type:</b>	Research Paper
<b>Section/Category:</b>	Environmental Chemical Engineering
<b>Keywords:</b>	cryogel; adsorption; heavy metals; N-methyl-D-glucamine; water purification; sequestration
<b>Corresponding Author:</b>	Martina Ussia Istituto per la Microelettronica e Microsistemi Consiglio Nazionale delle Ricerche CATANIA, ITALY
<b>First Author:</b>	Tommaso Mecca
<b>Order of Authors:</b>	Tommaso Mecca Martina Ussia Daniele Caretti Francesca Cunsolo Sandro Dattilo Stefano Scurti Vittorio Privitera Sabrina carola Carroccio
<b>Abstract:</b>	<p>The design of novel cryo-spongy polymeric networks containing N-methyl-D-glucamine (NMG), was herein reported as a valuable system to boost the removal of arsenic and chromium metal ions from water. Macroporous materials were prepared via a facile freeze-drying method in water by using as co-monomers (4-vinylbenzyl)-N-methyl-D-glucamine (VbNMG) and 2-hydroxyethyl methacrylate (HEMA) at different percentages. The as-prepared sponges were characterized by spectroscopic, thermal and morphological analyses. Arsenic and chromium sequestration were studied in a static mode revealing excellent performance in terms of adsorption for all synthesized samples. In particular, the effect of initial metal ions concentration, kinetic profiles, the presence of interfering anions (phosphate and sulphate) as well as adsorption/desorption studies were carried out on the most performant cryogel VbNMG-100. Its equilibrium sorption results well fitted the Langmuir isotherm for both ions tested, showing a startling aptitude in arsenic (76.3 mg/g) as well as chromium (130.9 mg/g) sorption properties if compared with similar polymeric materials. An excellent reusability by a simple squeezing of the sponge for several times as well as recyclability after acid washing cycles were also proved.</p>
<b>Suggested Reviewers:</b>	Bruno F. Urbano burbano@udec.cl  Alice Mija alice.mija@unice.fr  Suprakas Sinha Ray sinharays@toyota-ti.ac.jp
<b>Opposed Reviewers:</b>	

Dear Editor,

enclosed with this letter you will find the submission of a manuscript entitled “Boosting heavy metals removal from water by reusable cryo-sponges based on N-methyl-D-glucamine” by T. Mecca, D. Caretti, F. Cunsolo, S. Dattilo, S. Scurti, V. Privitera, S. C. Carroccio and myself. This is an original version which is not previously submitted anywhere else and all authors have read and approved the final version of the paper.

As emphasized from the World Health Organization (WHO) in several reports and communications *the water safety and quality are fundamental to human development and well-being. Providing access to safe water is one of the most effective instruments in promoting health and reducing poverty.* ([https://www.who.int/water\\_sanitation\\_health/emergencies/en/](https://www.who.int/water_sanitation_health/emergencies/en/))

In this context, metals and metalloids are toxic in nature even at very low concentration, causing serious health illness from human beings to animals, affecting also aquatic system *via* agricultural overflow and industrial discharges.

The present manuscript describes a novel approach to eliminate arsenic (V) and chromium (VI) from water, reasonably applicable to other hazardous materials such as boron and cadmium since the chelating agent N-methyl-D-glucamine (NMG) is well known for its ability in sequestering such kind of metal oxyanions. The novelty consists in formulating NMG polymeric derivatives by a cryo-structuration to obtain macroporous sponges that showed superior performance in removing arsenic (V) and chromium (VI), if compared to similar materials.

Besides the high chelating ability (which is in most cases the only data reported), the materials were designed to ensure their practical use as well as a sustainable waste management: stability, re-use and regeneration.

In this work, it was demonstrated as NMG-based cryo-sponges were able to purify water *via* a simple squeeze process, presenting easy reusability and fast regeneration aptitude as well. Furthermore, the effect of initial metal ions concentration, kinetic profiles as well as the presence of interfering anions were addressed. Owing to the outstanding results obtained, the present paper is part of a patent already applied (“N-alkyl-D-glucamine based macroporous polymeric cryogel for sequestering and/or removing toxic contaminants” Application number: 102019000012339).

Based on this brief foreword, I would appreciate if you would consider the manuscript for publication in *Chemical Engineering Journal-Elsevier*.

Sincerely,

Dr. Martina Ussia  
CNR-IMM Ct Unit  
Via Santa Sofia 64, 95123  
Catania, Italy

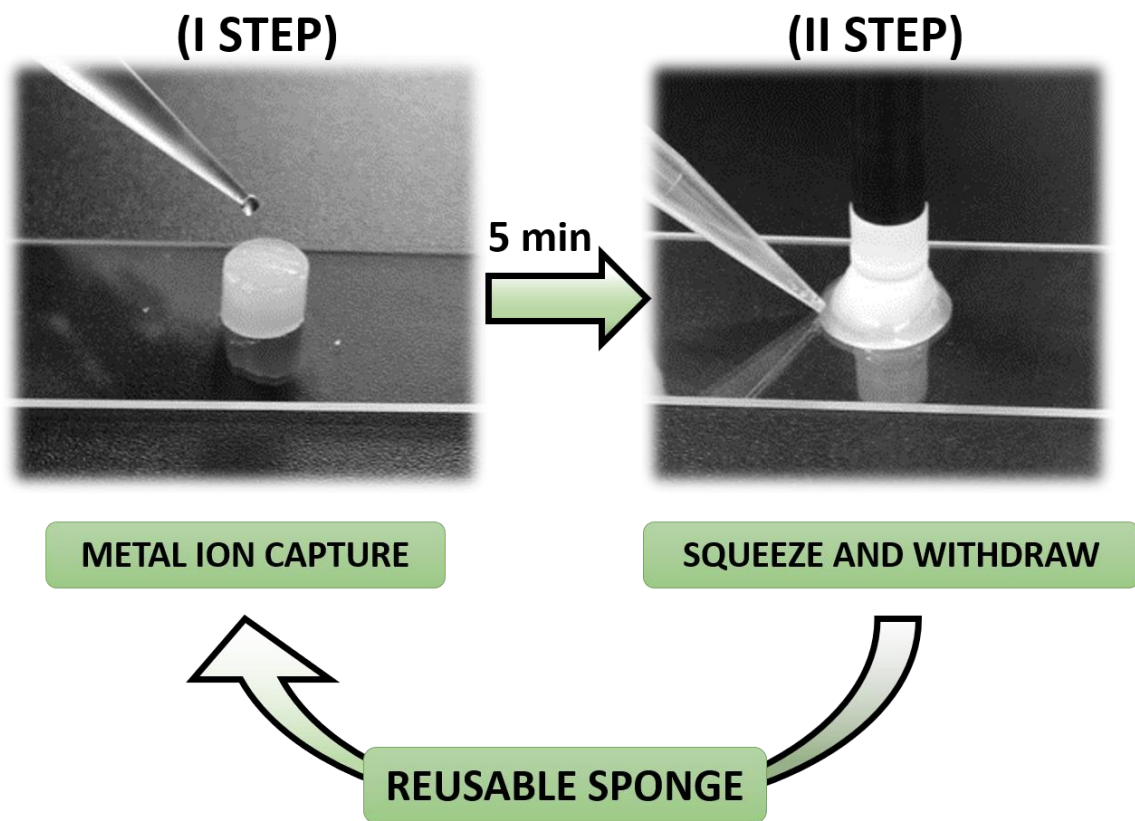
Dear Editor,

a list of suggested referees and contact details is provided as follows:

- Prof. Bruno F. Urbano, University of Concepción (Department of Polymers, Faculty of Chemical Sciences) [burbano@udec.cl](mailto:burbano@udec.cl)
- Prof. Alice Mija, University of Sophia Antipolis (Nice, France) [alice.mija@unice.fr](mailto:alice.mija@unice.fr)
- Prof. Suprakas Sinha Ray, (Advanced Polymeric Materials Engineering, Graduate School of Engineering, Toyota Technological Institute) [sinharays@toyota-ti.ac.jp](mailto:sinharays@toyota-ti.ac.jp)

Sincerely,

*Dr. Martina Ussia*  
CNR-IMM Ct Unit  
Via Santa Sofia 64, 95123  
Catania, Italy



- Facile cryo-polymerization in water of N-methyl-D-glucamine derivatives were designed.
- Macro-porous polymer network boosts the heavy metals ions uptake.
- Purified water was obtained by simple squeezing the sponge's materials.
- Cryo-sponges can be easily reused and regenerated as well.

# Boosting heavy metals removal from water by reusable cryo-sponges based on N-methyl-D-glucamine

Tommaso Mecca<sup>a</sup>, Martina Ussia<sup>\*b</sup>, Daniele Caretti<sup>c</sup>, Francesca Cunsolo<sup>a</sup>, Sandro Dattilo<sup>d</sup>, Stefano Scurti<sup>c</sup>, Vittorio Privitera<sup>b</sup>, Sabrina C. Carroccio<sup>b,d</sup>

<sup>a</sup> CNR-ICB, Via Paolo Gaifami 18, 95126, Catania, Italy.

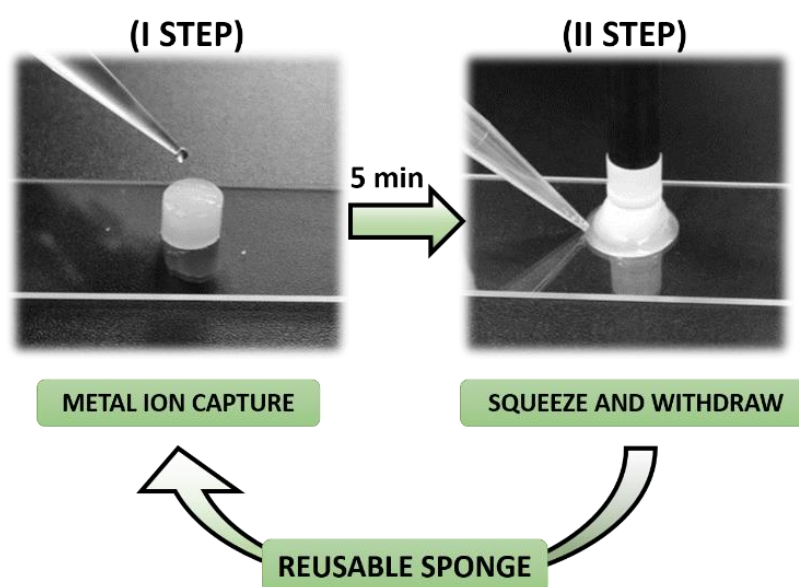
<sup>b</sup> CNR-IMM, Via Santa Sofia 64, 95123, Catania, Italy.

<sup>c</sup> Industrial Chemistry "Toso Montanari" Department, University of Bologna, Viale Risorgimento 4, 40136, Bologna, Italy.

<sup>d</sup> CNR-IPCB, Via Paolo Gaifami 18, 95126, Catania, Italy.

**Keywords:** adsorption, water remediation, hydrogel, heavy metal, kinetic, polymer, N-methyl-D-glucamine, sequestration

\*Correspondence to: [martina.ussia@ct.infn.it](mailto:martina.ussia@ct.infn.it)



**Authors contribution:** S. C. Carroccio and D. Caretti conceived the project idea. D. Caretti and S. Scurti synthesized the monomer performing NMR and FT-IR analyses. M. Ussia, T. Mecca and F. Cunsolo synthesized the cryo-sponges. M. Ussia and T. Mecca performed adsorption tests. T. Mecca carried out porosity tests. M. Ussia achieved, analysed and discussed SEM images as well as adsorption, kinetic and recycling measurements. S. Dattilo and S. C. Carroccio performed and discussed the ICP-MS and TGA measurements. M. Ussia and S. C. Carroccio wrote the paper; V. Privitera and F. Cunsolo reviewed and commented on the manuscript at all stages; Sabrina C. Carroccio supervised all work stages.

## Abstract

The design of novel cryo-spongy polymeric networks containing N-methyl-D-glucamine (NMG), was herein reported as a valuable system to boost the removal of arsenic and chromium metal ions from water. Macroporous materials were prepared via a facile freeze-drying method in water by using as co-monomers (4-vinylbenzyl)-N-methyl-D-glucamine (VbNMG) and 2-hydroxyethyl methacrylate (HEMA) at different percentages. The as-prepared sponges were characterized by spectroscopic, thermal and morphological analyses. Arsenic and chromium sequestration were

1 studied in a static mode revealing excellent performance in terms of adsorption for all synthesized  
2 samples. In particular, the effect of initial metal ions concentration, kinetic profiles, the presence of  
3 interfering anions (phosphate and sulphate) as well as adsorption/desorption studies were carried out  
4 on the most performant cryogel VbNMG-100. Its equilibrium sorption results well fitted the  
5 Langmuir isotherm for both ions tested, showing a startling aptitude in arsenic (76.3 mg/g) as well as  
6 chromium (130.9 mg/g) sorption properties if compared with similar polymeric materials. An  
7 excellent reusability by a simple squeezing of the sponge for several times as well as recyclability  
8 after acid washing cycles were also proved.  
9  
10  
11  
12  
13  
14  
15

## 16 **1. Introduction**

17 The global demand for the access to clean water constitutes one of the urgent challenges to be faced  
18 in the next future [1,2]. As water pollutants, heavy metals play a major role, since their presence in  
19 water sources drastically increased in the past decades, causing serious threat for aquatic and human  
20 health. Particularly, arsenic V [As(V)] and chromium VI [Cr(VI)] are included amongst the most  
21 hazardous species, so that their level of contamination is strictly regulated by health authorities,  
22 recommending a limit content in drinking water of 10 µg/L and 50 µg/L for As(V) and Cr(VI),  
23 respectively [3-6]. However, even though these levels are maintained in Europe and USA, emerging  
24 countries population are exposed to considerable higher amount of metal ions in drinking water [6-  
25 8]. Indeed, metal contamination in ground and surface waters deriving from anthropogenic activities  
26 is scarcely regulated due to missing or unacceptably inadequate environmental control. Therefore,  
27 researchers have addressed their efforts in the identification of suitable and cost-effective  
28 technologies for their removal [2, 9-22].  
29  
30  
31  
32  
33  
34  
35  
36  
37  
38  
39

40 As well known, the adsorption is the most widely used technology, consisting in simple and low-cost  
41 handling procedures to remove organic and inorganic contaminants from water [2, 23-26] avoiding  
42 at the same time the use of chemical reagents as well as the production of harmful by-products  
43 downstream [27].  
44  
45  
46

47 In this context, hydrogels have become a crucial component of novel smart adsorbent materials for  
48 several applications including water remediation [15,28-30]. Specifically, hydrogels with a three-  
49 dimensional porous structure as well as specific functional moieties (such as carboxylic, amine,  
50 hydroxyl, or sulfonic acid groups along their polymeric chains), are able to trigger the sequestration  
51 of metal ions from contaminated aqueous medium, resulting in stable complexes with them.  
52 Hereafter, the linked contaminants can be released from the network by simply changing  
53 environmental conditions such as pH, thus regenerating the polymer network. In view of this, together  
54 with a desirable increment in terms of efficiency and selectively versus specific elements, these  
55  
56  
57  
58  
59  
60  
61  
62  
63  
64  
65

1 promising materials need to face significant improvements before their transfer into the market,  
2 especially in terms of their sustainability, as well as chemical and mechanical resistance during the  
3 regenerating treatments cycles. As a consequence, cost- and time-saving polymerizations of common  
4 bio-based as well as synthetic acrylic and vinylic materials functionalized *ad hoc* with chelating  
5 groups, was widely reported to achieve resistant and efficient materials. Specifically, huge attention  
6 was devoted to N-methyl-D-glucamine (NMG) functional group due to its high efficiency and  
7 selectivity versus metal ions species [31-45]

8 Monomers containing NMG can be successfully polymerized in situ by radical initiators [31-39] or  
9 alternatively, NMG can be grafted to the material surface after the polymerization step [40-44].

10 Herein, we reported as a novelty, the syntheses in water of macroporous hydrogels produced by a  
11 cryogenic treatment. Specifically, cryogels were formulated starting from (4- vinylbenzyl)- N-  
12 methyl- D- glucamine (VbNMG) and HEMA monomers. This unusual choice to develop spongy  
13 materials *via* cryo-polymerization was adopted assuming that the typical high internal porosity and  
14 specific surface area of macroporous structure could assist in boosting metal ions adsorption.  
15 Moreover, the resulted water-insoluble cryogels can be easily compressed for several cycles to a very  
16 small volume facilitating both reuse and disposal, releasing purified water by a simple squeezing.  
17 Synthesized polymer sponges were characterized by Fourier transform infrared (FTIR) spectroscopy,  
18 thermogravimetric analysis (TGA), as well as scanning electron microscopy (SEM). Their adsorption  
19 capability, contact time and recyclability were finally tested. Data obtained in terms of As(V) and Cr  
20 (VI) removal were here discussed and compared with those reported in literature [31,39,41] including  
21 also commercial NMG-based macroporous resins [41,42].

## 2. Experimental part

### 2.1 Materials

22 2-Hydroxyethylmethacrylate (HEMA), N,N'-methylene-bis-acrylamide (MBAA), ammonium  
23 persulfate (APS), tetramethyl-ethylene-diamine (TEMED), sodium arsenate dibasic heptahydrate  
24 ( $\text{Na}_2\text{HAsO}_4 \cdot 7\text{H}_2\text{O}$ ), potassium dichromate ( $\text{K}_2\text{Cr}_2\text{O}_7$ ), absolute ethanol (EtOH), hydrochloric acid  
25 (37%) were purchased from Sigma Aldrich. (4- Vinylbenzyl)- N- methyl- D- glucamine  
26 (VbNMG) was synthesized in our laboratories.

### 2.2 Synthesis of (4- vinylbenzyl)- N- methyl- D- glucamine (VbNMG)

27 The starting monomer was synthesized by suspending NMG (1 g, 5 mmol) in 30 ml of  $\text{CH}_3\text{OH}$  and  
28 adding to the suspension an equimolar amount of 4-vinyl-benzylchloride (0.70 mL, 5 mmol) in  
29 presence of  $\text{Na}_2\text{CO}_3$ , according to the reaction reported in **Figure S1**. The reaction mixture was stirred  
30  
31  
32  
33  
34  
35  
36  
37  
38  
39  
40  
41  
42  
43  
44  
45  
46  
47  
48  
49  
50  
51  
52  
53  
54  
55  
56  
57  
58  
59  
60  
61  
62  
63  
64  
65



1  
2  
3  
4  
5  
6  
7  
8  
9  
10  
11  
12  
13  
14  
15  
16  
17  
18  
19  
20  
21  
22  
23  
24  
25  
26  
27  
28  
29  
30  
31  
32  
33  
34  
35  
36  
37  
38  
39  
40  
41  
42  
43  
44  
45  
46  
47  
48  
49  
50  
51  
52  
53  
54  
55  
56  
57  
58  
59  
60  
61  
62  
63  
64  
65

at room temperature monitoring the reaction progress by Thin Layer Chromatography (TLC). At the end, the mixture was filtered and the methanol evaporated. The product was purified by crystallization in CHCl<sub>3</sub> and characterized by Nuclear Magnetic Resonance (see **Figure S2** and **Figure S3**).

### 2.3 Synthesis of VbNMG-based polymers by cryopolymerization

In a 1.5 mL vial containing 180  $\mu$ L of H<sub>2</sub>O, 40 mg of (4- vinylbenzyl)- N- methyl- D- glucamine (Vb-NMG) and 3.3 mg of N,N'-methylene-bis-acrylamide (MBAA, molar ratio 1/6 comparing to the moles of monomer) were added. Syntheses of copolymers were performed adding HEMA as co-monomer using following the VbNMG/HEMA molar ratio : 25/75, 50/50, 75/25. HCl 2N was added in small doses to the reaction mixture under vigorous stirring, controlling the pH up to the neutrality (about 50  $\mu$ L). Additional 24  $\mu$ L of H<sub>2</sub>O were added, then the solution was cooled to 0 °C and 3  $\mu$ L of a 10% w/v ammonium persulphate (APS) solution in water and 3  $\mu$ L of a 10% w/v tetramethyl-ethylene-diamine (TEMED) solution in water were added respectively under vigorous stirring. The reaction mixture was stirred for about 1 min and then transferred to a glass micro-reactor with a diameter of about 5.5 mm pre-cooled to 0 °C. The reactor was placed in a cryostat at -14 °C for about 24 hours, then, after thawing, the cryogel obtained was washed with mixtures of H<sub>2</sub>O/HCl/EtOH progressively increasing the concentration of EtOH up to pure EtOH. The purified cryogel was dried under nitrogen flow and then under vacuum. The final product consists of macroporous monolithic cryogel. The yield of reactions ranges from 80 to 85 %.

### 2.4 Characterizations

All the synthesized materials were accurately characterized. The VbNMG monomer structure was confirmed by <sup>1</sup>H and <sup>13</sup>C spectra, registered by using Varian “Mercury 400” and “Mercury 600” spectrometers, operating at 400 and 600 MHz, respectively. TMS was used as reference.

All formulated samples were characterized by fourier transform infrared spectroscopy (FTIR) spectroscopy, and the spectra were acquired through a PerkinElmer Spectrum 1000 spectrometer.

Morphologies of the sponges were investigated by scanning electron microscopy (SEM), performed by using a Zeiss Supra 25 field emission microscope. All samples were previously coated with a thin layer of gold (<10 nm) in order to make them conductive.

Samples were subjected to thermogravimetric analyses (TGA) by using a thermogravimetric apparatus (TA Instruments Q500) under nitrogen atmosphere (flow rate 60 mL/min) at 10 °C/min heating rate, from 40 °C to 800 °C. TGA sensitivity is 0.1 $\mu$ g with a weighting precision of  $\pm$  0.01%. The isothermal temperature accuracy is  $\pm$  1°C.

Swelling tests were performed on dried cylindrical samples (4mm×9mm). After water uptake and removal of its surplus from the surface, mass measurements were performed. The total water uptake for all samples was determined by calculating the increase of cumulative mass at a fixed time intervals. The equilibrium swelling degree was measured weighting the wet sample immersed in water for 30 min, whereas, the adsorption kinetic was estimated after keeping the samples in contact with a slight excess of water for selected times, followed by quick removal of the excess of unabsorbed water. The adsorbed water was evaluated by weight the sample in function of the time, normalizing all data. Swelling–deswelling cycles performance were evaluated on about 20 mg of wet samples. All samples were kept in contact with water and weighted after 5 min of contact time. Then all samples were squeezed between two paper foils until to water residue was removed. After that samples were weighted and kept once more in water to repeat the squeezing procedure up to 5 times. The equilibrium swelling degree can be calculated using the following formula [45].

$$\text{Swelling degree} = \frac{(m_w - m_d)}{m_d} \quad (1)$$

where  $m_w$  is the weight of the wet cryogel and  $m_d$  is the weight of the dry cryogel.

The porosity of the dried sample was determined from eq. (2), by measuring the absorbed volume of cyclohexane versus the total volume of each sample using a pycnometer.

$$\text{Porosity \%} = \frac{V_{pores}}{V_{sample}} 100 = \frac{m_w - m_d}{m_1 - m_2 + m_w} 100 \quad (2)$$

where  $m_d$  is the mass of dried cryogel,  $m_w$  is the mass of the cryogel wet in cyclohexane,  $m_1$  is the mass of the apparatus filled with cyclohexane,  $m_2$  is the mass of the apparatus with cyclohexane plus cryogel [46]. Before each measurement, residual gas entrapped into the cryogel was removed under reduced pressure.

Quantitative determination of metal ions in solution after sequestration procedure, was performed by an Inductively coupled plasma–mass spectrometry (ICP/MS) Nexion 300X (Perkin Elmer Inc. Waltham, Massachusetts, U.S.A.) using the kinetic energy discrimination mode (KED) for interference suppression. Each determination was performed three times. The accuracy of the analytical procedure was confirmed by measuring a standard reference material, Nist 1640a trace element in natural water, without observing an appreciable difference.

Batch equilibrium tests were carried out to calculate the equilibrium retention capacity ( $Q_e$ ) values as well as the metal ions removal percentage. In general, ~10 mg of cryo-sponges were immersed into either chromium ( $K_2Cr_2O_7$ ) or arsenate ( $Na_2HAsO_4 \cdot 7H_2O$ ) solutions (5 mL and pH=6) at different initial concentration, ranging from 30 to 1400 mg/L. The vials were maintained under constant

1 shaking at 25°C and 180 rpm for 24h, withdrawing aliquots of 100 µL at different interval time to  
2 perform kinetic studies. The residual metal ion concentrations were evaluated by ICP-MS  
3 measurements.  
4

5  
6 For the interfering tests, several samples containing 30 mg/L of arsenate ions and either sulphate or  
7 phosphate ions at different concentrations (ranging from 0 to 480 mg/L) were prepared. A few  
8 milligrams of VbNMG-100 sponge were added to each solution and the samples were shaken for 24h  
9 at 25°C and 180 rpm.  
10  
11

12  
13 To study the reusability of VbNMG-100, materials were subjected to six consecutive  
14 adsorption/desorption cycles. Specifically, 30 mg/L of arsenate solution was added drop by drop to  
15 ~134 mg of sponge to reach the maximum swollen degree. After 5 minutes of contact time the sponge  
16 was squeezed, withdrawing arsenate solution. Then, the sample was kept between two foils of  
17 cellulose paper for 10 minutes to remove the excess of arsenate solution before adding the fresh one.  
18 The As(V) residue collected after each cycle was measured by ICP-MS.  
19  
20  
21  
22  
23  
24

25 To evaluate the complete regeneration of cryo-sponge, recycling tests by washing in acidic media the  
26 sample was carried out. To this purpose, the material was kept in contact for 24h with 1400 mg/L of  
27 arsenate solution. After that, the sponge was regenerated in column with HCl 1M and washed with  
28 water to reach pH=6. The experiment was repeated up to three subsequent cycles. After each cycle  
29 both acid and residue arsenate solutions were analysed by ICP-MS.  
30  
31  
32  
33  
34

35 Three different semi-empirical adsorption kinetic models were used to study and analyze the kinetic  
36 performance in As(V) and Cr(VI) adsorption: pseudo-first order, pseudo second-order and  
37 intraparticle diffusion models [47]. Based on the adsorption equilibrium capacity ( $Q_e$ ) calculated by  
38 the following equation:  
39  
40  
41

$$42 \quad Q_e = \frac{(C_0 - C_e) \times V}{W} \quad (3)$$

43 where  $C_0$  (mg/L) is the metal initial concentration,  $C_e$  (mg L<sup>-1</sup>) is the concentration at the equilibrium,  
44 V (L) is the volume of water, W (g) is the weight of adsorbent used during the adsorption experiments.  
45

46 Lagergren pseudo-first order model for heterogeneous solid-liquid systems is formulated as follows:  
47  
48

$$49 \quad \ln(Q_e - Q_t) = \ln Q_e - k_1 t \quad (4)$$

50 where  $Q_e$  and  $Q_t$  (mg/g) are the amount of metal ions adsorbed at equilibrium and time  $t$  (min),  
51 respectively, by using as initial conditions  $Q_t = 0$  at  $t = 0$ ,. The slope value obtained by plotting  $\ln(Q_e -$   
52  $Q_t)$  versus time (min) (Figure 5(a)), allows to estimate the constant rate  $k_1$  (min<sup>-1</sup>).  
53  
54

55 Besides eq. (2), the pseudo-second order model allows to calculate the reaction rate  $k_2$  (g mg<sup>-1</sup>min<sup>-1</sup>),  
56 given by the following equation:  
57  
58  
59  
60  
61  
62  
63  
64  
65

$$\frac{t}{Q_t} = \frac{1}{k_2 Q_e^2} + \frac{t}{Q_e} \quad (5)$$

By plotting the experimental data  $t/q$  versus  $t$ ,  $Q_e$  and  $k_2$  were assessed from both slope and intercept, respectively (see Table 3).

As well stated, the pseudo-second order equation, better describes the entire metal ions adsorption process than the pseudo-first-order model, which is more useful to describe the first 20-30 minutes of adsorption process [47,48]. On the other hand, eq. (3) can indicate if a chemisorption process occurs taking into account the adsorbent-adsorbate interactions [47].

The intraparticle diffusion model is described with the following equation:

$$Q_t = k_i \sqrt{t} + C \quad (6)$$

where  $k_i$  is the intraparticle diffusion rate constant ( $\text{mg g}^{-1} \text{h}^{-0.5}$ ).

One of the most important isotherm adsorption model to obtain useful information about the adsorbate/adsorbent interaction is described by the Langmuir model equation [49].

The Langmuir equation is:

$$q_e = \frac{Q_0 b C_e}{1 + b C_e} \quad (7)$$

where  $q_e$  ( $\text{mg g}^{-1}$ ) is the amount of metal ions adsorbed per unit weight of adsorbate,  $C_e$  ( $\text{mg L}^{-1}$ ) is the metal concentration at the equilibrium,  $Q_0$  ( $\text{mg g}^{-1}$ ) is the monolayer capacity and  $b$  ( $\text{mg}^{-1} \text{L}$ ) represents the constant associated to adsorption heat.

### 3. Results and Discussion

#### 3.1 Cryogels synthesis and characterization

High-quality chelating polymeric materials for water remediation should be designed considering several factors including high surface area and pore size, mechanical and chemical stabilities, high and fast adsorption efficiency. Their recyclability as well as environmental sustainability, are also required. In this work, sponges based on VbNMG and different percentages of HEMA (from 0 to 75%) were synthesized *via* cryostructuring method in water at temperature below its freezing point (see **Figure 1**). The synthesized samples were named depending on the VbNMG percentage content as VbNMG-100, VbNMG-75, VbNMG-50 and VbNMG-25 (for example, Vb-NMG-25 refers to the sample with 25% Vb-NMG and 75% HEMA). All prepared cryo-sponges were subjected to spectroscopical (see FT-IR in supporting informations), morphological and thermal characterizations as well as porosity and swelling tests as reported as follows.

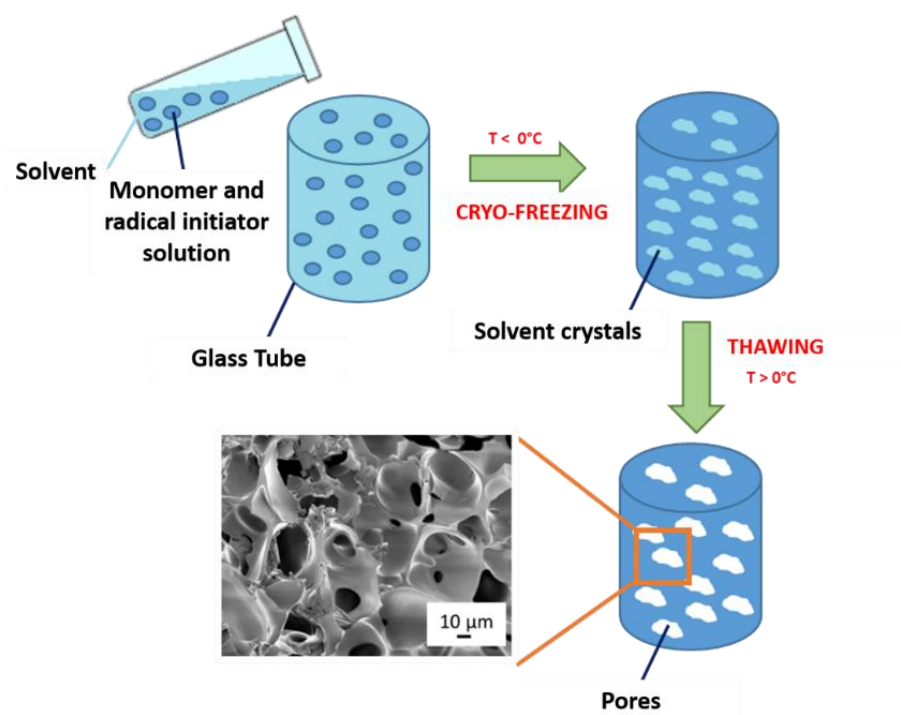


**Figure 1.** Schematic diagram of VbNMG cryogels synthetic procedure.

### 3.2 SEM Analyses

The morphology of the VbNMG polymeric sponges and related copolymers was studied by scanning electron microscopy (SEM), and the micrographs reported in **Figure 2 (a-d)**. As expected all cryogels samples showed a typical macroporous structure. In particular, **Figure 2 (a)** revealed that the VbNMG-100 cryogel is consisted of a uniform and regular pore distribution ranging from 20 to 30  $\mu\text{m}$ . Vice versa, cryogel with an higher content of HEMA [**Figures 2(b), (c) and (d)**] exhibited a more jagged porous structure with smaller pore size distributions. From the inspection of the high-magnification images [see insets of **Figures 2 (a)-(d)**], it is possible to appreciate that the shape as well as the pores distribution observed was strongly influenced from the increasing HEMA content added during the cryo-polymerization.

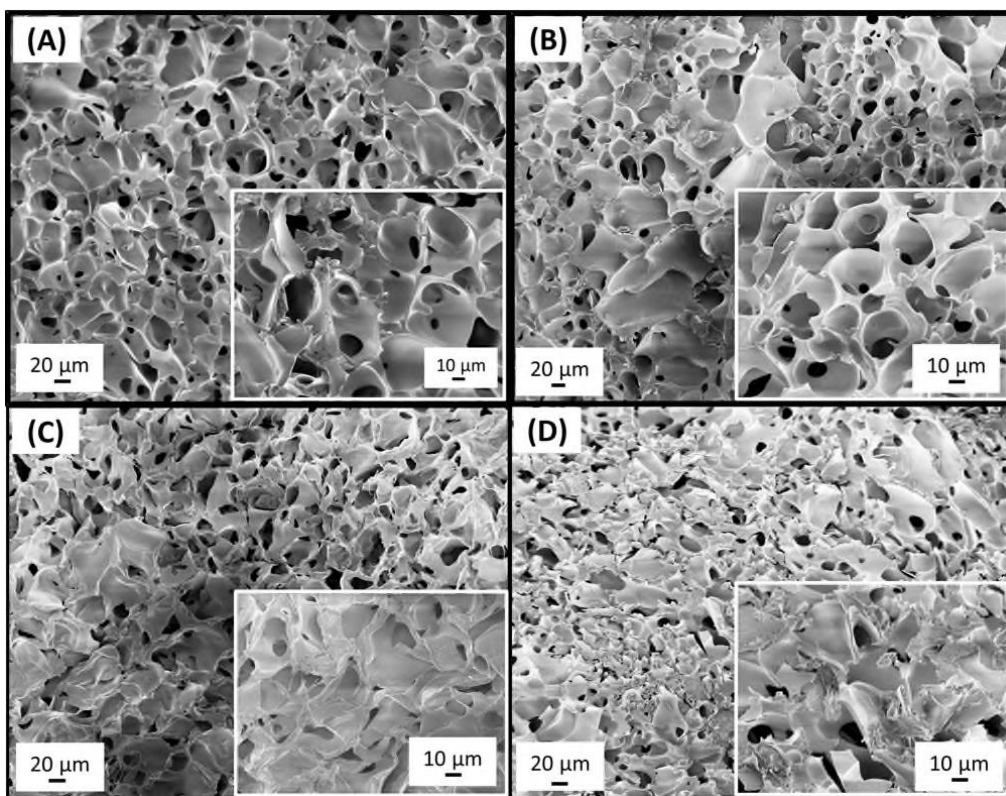


**Figure 2.** SEM images of (a) VbNMG-100, (b) VbNMG-75, (c) VbNMG-50 and (d) VbNMG-25.

### 3.3 Thermogravimetric analyses (TGA)

**Table 1** showed the TGA of (4-vinylbenzyl)-N-methyl-D-glucamine polymer and the related copolymers containing 25, 50 and 75% of HEMA. All samples undergo to two separate thermal degradation steps beginning from  $\sim 200^{\circ}\text{C}$  up to  $\sim 500^{\circ}\text{C}$ .

**Table 1.** Temperatures at maximum rate of decomposition and residual masses of NMG samples containing different amounts of HEMA: 0% (VbNMG-100), 25% (VbNMG-75), 50% (VbNMG-50) and 75% (VbNMG-25).

	VbNMG-100	VbNMG-75	VbNMG-50	VbNMG-25
<b>I degradation step (<math>^{\circ}\text{C}</math>)</b>	280.9	273.9	274.3	265.4
<b>II degradation step (<math>^{\circ}\text{C}</math>)</b>	425.4	417.2	415.8	412.3
<b>Residue %</b>	15.2	6.0	5.5	0.5

In agreement with the literature [50], the first thermal degradation step can derive from the decomposition of glucamine chelating groups of the cryogel, whose temperatures at maximum rate of decomposition (TMD) decreased with increasing of HEMA content. At higher temperature, the thermal degradation of poly 4-vinyl-benzyl chain as well as HEMA moieties took place, giving TMD in the range of  $412 - 425^{\circ}\text{C}$ . As expected, the residue increased as a function of the aromatic content due to the formation of insoluble gel.

### 3.4 Porosity tests

The porosity of all synthesized cryogels was measured. Specifically, the porosity values were calculated following the equation (2) reported in the experimental section. The obtained data reported in **Figure 3** evidenced that the porosity of VbNMG polymer and copolymers was not significantly affected by the addition of increasing amounts of HEMA co-monomer.

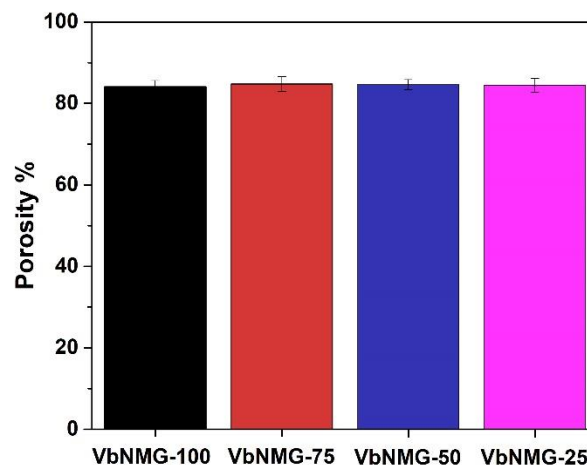


**Figure 3.** Porosity of the prepared VbNMG cryogels expressed as a function of the percentage of absorbed volume of cyclohexane.

### 3.5 Swelling degree tests

In **Figure 4 (a-b)** the equilibrium swelling degree (ESD) tests as well as swelling/deswelling degree cycles were reported. The column bars of **Figure 4 (a)** showed that ESD values follows the order  $VbNMG-100 > VbNMG-75 \approx VbNMG-50 > VbNMG-25$ , with ESD values included in the range  $18,2 \pm 0,9$  and  $15,8 \pm 1,4$  g/g. The obtained results indicated that the VbNMG-100 cryogel is able to absorb higher amounts of water. This finding is in good agreement with data obtained from SEM images. Specifically, the smaller pore sizes obtained by introducing higher amount of HEMA co-monomer slightly affected the water diffusion, and thus the ESD values. Nevertheless, although VbNMG copolymers presented lower water uptake, all samples preserved almost constant the swelling/deswelling ability up to 5 cycles [see **Figure 4 (b)**].

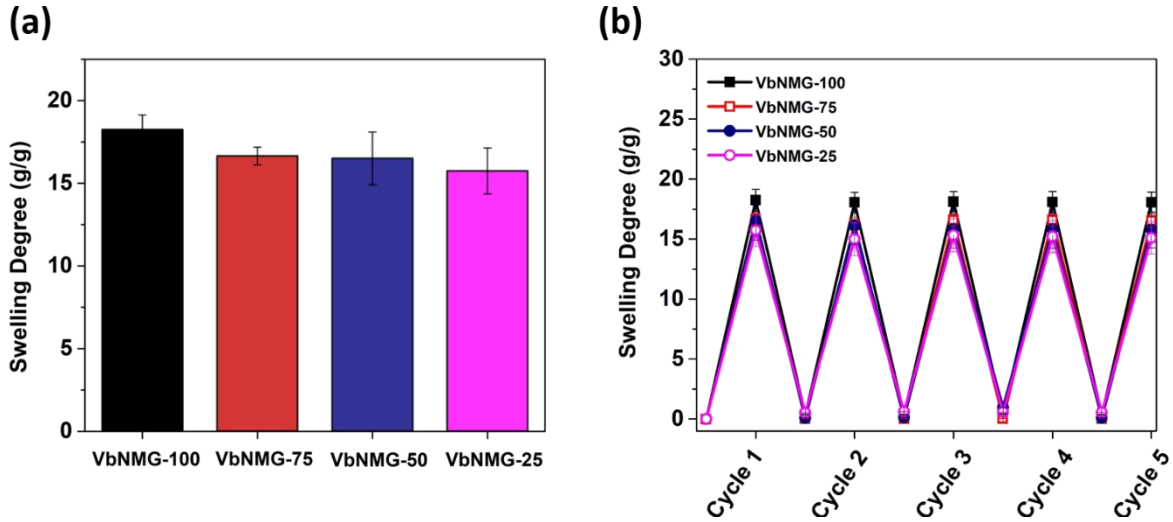


**Figure 4.** (a) Equilibrium swelling degree and (b) Swelling/deswelling cycles of VbNMG samples.

### 3.6 As(V) and Cr(VI) adsorption studies

Preliminary tests to evaluate the adsorption ability versus As(V) and Cr(VI) of the cryogels depending on their HEMA content were carried out. In particular, metal ions solutions with a 45 ppb concentration were tested by using ~ 8 mg of sample.

As it is possible to appreciate from **Table 2**, all VbNMG-based materials were able to reduce the As as well as Cr concentration below 10  $\mu\text{g/L}$ . Specifically, after 8h of contact time, VbNMG-100 showed the best performance with metal ion residues in water of 1.9  $\mu\text{g/L}$  and 0.7 for As(V) and Cr(VI), respectively. Besides, in view of industrial applications of cryo-sponges in filtering systems and depending on the ion contents to be removed, their sorption capability can be tuned. Indeed, by changing the % of HEMA added during the synthesis it is possible to modulate the sequestrant power assuring also a water swelling aptitude.

**Table 2.** Preliminary tests of As(V) and Cr(VI) removal on NMG cryogels with different HEMA content.

	$C_0$ of As(V) and Cr(VI) <sup>a</sup> ( $\mu\text{g/L}$ )	$C_{8h}$ As(V) <sup>b</sup> ( $\mu\text{g/L}$ )	$C_{8h}$ Cr(VI) <sup>b</sup> ( $\mu\text{g/L}$ )
<b>VbNMG-100</b>	45	1.9	0.7
<b>VbNMG-75</b>	45	4.0	1.5
<b>VbNMG-50</b>	45	7.1	2.9
<b>VbNMG-25</b>	45	9.8	5.5

**a**  $C_0$  is the initial concentration of metal ion

**b**  $C_{8h}$  is the final concentration of metal ion after 8h of contact time



Based on these excellent results, concentration effect, kinetic profiles studies, interfering ion tests as well as sorption/desorption capacity of the most performant VbNMG-100 cryogel were carried out.

### 3.6.1 Concentration effects

To quantify the capacity of VbNMG-100 cryogel for the removal of As(V) and Cr(VI) from water as a function of the concentration effect, batch equilibrium procedures was carried out. Six different metal ions solutions were selected with a concentration significantly higher than the permitted WHO limits and by using no more than 11 mg of cryo-sponge for each batch experiment. **Table 3** reports the initial concentrations of metal ion ( $C_0$ ), the measured concentration at the equilibrium ( $C_e$ ), the normalized equilibrium capacity ( $Q_e$ ) and the calculated percentage of metal ion retention after 24h of contact time at room temperature and pH=6.

**Table 3.** Initial concentration of metal ions ( $C_0$ ), at the equilibrium ( $C_e$ ), equilibrium removal capacity ( $Q_e$ ), and percentage of metal ions removal after 24 h of contact time at room temperature.

As(V)				Cr(VI)			
$C_0$ (mg L <sup>-1</sup> )	$C_e$ (mg L <sup>-1</sup> )	$Q_e$ (mg g <sup>-1</sup> )	Retention <sup>a</sup> %	$C_0$ (mg L <sup>-1</sup> )	$C_e$ (mg L <sup>-1</sup> )	$Q_e$ (mg g <sup>-1</sup> )	Retention <sup>a</sup> %
7.7	0.3	4.2	97.65	7.9	0.1	10.2	98.53
17.4	0.5	7.7	97.27	18.1	0.2	18.3	98.87
72.6	1.5	36.5	97.87	68.3	1.3	59.9	98.12
168.4	18.6	69.4	88.97	165.1	10.7	122.5	93.50
338.8	182.5	73.7	46.17	308.1	190.2	125.4	37.15

<sup>a</sup>  $\frac{(C_0 - C_e)}{C_0} \times 100$

As it is possible to see from **Table 3**, all batch experiments showed highly efficient removal of both As(V) and Cr(VI) for all concentration studied, excepted for the highest ones, due to the reaching of cryo-sponge saturation limit.

### 3.6.2 As(V) and Cr(VI) adsorption kinetic profiles

To determine the adsorption equilibrium time, kinetic profiles were determined [see **Figure 5(a-b)**]. For both metal ions all experiments were carried out at different initial concentrations and exhibited similar adsorption trends, denoting noteworthy increments for the first 2 hours that level after 6h, reaching the equilibrium time after about 7h. Furthermore, an increase in the cryogel adsorptive capacity was observed for Cr(VI) if compared to the As(V) removal performance.

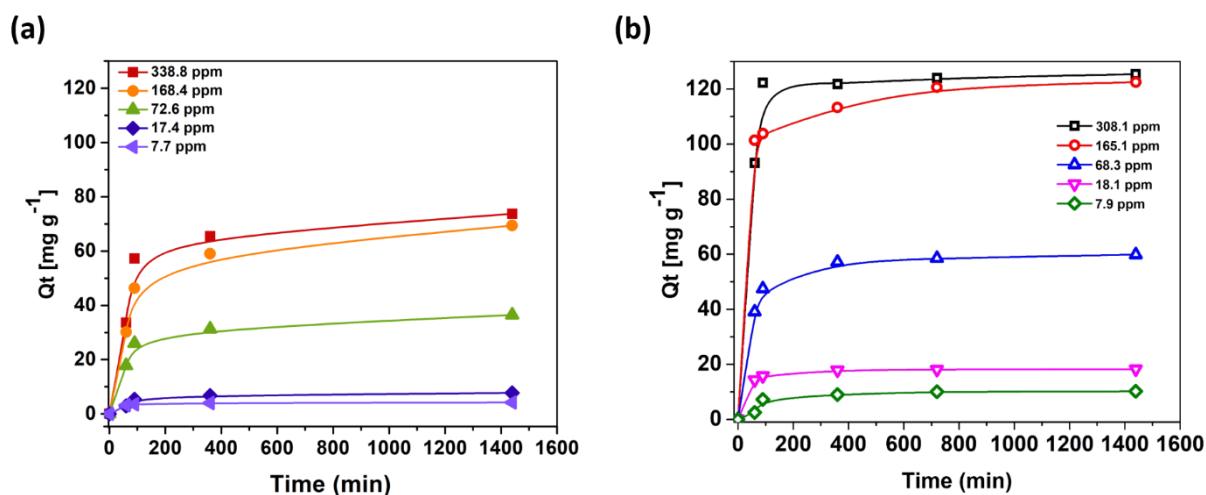


**Figure 5.** Kinetic profiles of (a) As(V) and (b) Cr(VI) adsorption calculated for different metal ion concentrations.

From kinetic point of view, three different models were used (see experimental section and **Figure S6** and **Figure S7**). In particular, by applying the pseudo-second order model and comparing the extrapolated R-square ( $R^2$ ), excellent fits for both metal ions were obtained at all tested concentrations. Further proof of this result, was evidenced from the comparison between the theoretical adsorption capacity values ( $Q_{eT}$ ) with those obtained experimentally (see **Table 4** for both metal ions). Specifically,  $Q_{eT}$  derived from equation (3) well matched the experimental values ( $Q_{exp}$ ), differently to those obtained from equation (2) (see experimental section). The deviance from the linearity of the pseudo-first order model attributed to an intense initial adsorption process as well as the best fit with the pseudo-second order model, allow to assume that the rate-limiting step is the surface adsorption of As(V) and Cr(VI) ions that involve chemisorption [39,51]. According to the literature, at the operating pH ( $\sim 6$ ) the adsorption is controlled by both electrostatic and hydrogen bonding interactions between VbNMG and As(V) anionic forms ( $H_2AsO_4^-$  and  $HAsO_4^{2-}$ ) and Cr(VI) anionic forms ( $HCrO_4^-$  and  $CrO_4^{2-}$ ) [31,39,42,52,53]. Particularly, electrostatic attraction is driven by the protonated tertiary amine, whereas OH groups can promote hydrogen linkages.

As regards the constant rates, it was observed that the  $K_2$  values decreased with increasing initial metal ions concentrations (see **Table 3**). This finding suggested that higher concentrations of metal ions might cause adsorbate surface saturation, in agreement with the lower retention percentage evidenced in the previous section. As a result, a dropping off in diffusion rate of metal ions occurred. Indeed, deviation from the linearity of the intraparticle diffusion model (see **Table 3**) was also observed [**Figure S6 (c)** and **Figure S7 (c)**].

**Table 3.** Kinetic parameters calculated from pseudo-first order, pseudo-second order and intraparticle diffusion models for As(V) and Cr(VI) adsorption experiments.

	As(V)					Cr(VI)				
$C_0$	338.8	168.4	72.6	17.4	7.8	308.1	165.1	68.3	18.1	7.9
$Q_{exp}$ (mg g <sup>-1</sup> )	73.7	69.4	36.5	7.7	4.2	125.4	122.5	59.9	18.3	10.2
	I order					I order				
$K_1 \times 10^{-3}$ (min <sup>-1</sup> )	5.95	5.04	5.10	5.79	7.18	4.71	4.62	4.76	6.01	5.72
$R^2$	0.93	0.97	0.93	0.99	0.82	0.43	0.79	0.82	0.81	0.96
$Q_{eT}$ (mg g <sup>-1</sup> )	61.72	60.5	30.03	7.11	2.64	29.55	47.90	28.85	6.77	8.42
	II order					II order				
$K_2 \times 10^{-3}$ (min <sup>-1</sup> )	0.28	0.56	1.55	4.84	25.5	0.85	0.56	0.82	5.35	1.24
$R^2$	0.99	0.99	0.99	0.99	0.99	0.99	0.99	0.99	0.99	0.99
$Q_{eT}$ (mg g <sup>-1</sup> )	75.82	70.37	36.81	7.84	4.2	125.94	123.30	60.57	18.38	10.80
	Intraparticle diffusion					Intraparticle diffusion				
$R^2$	0.57	0.69	0.63	0.66	0.36	0.36	0.41	0.54	0.41	0.69
$K_{ip}$	1.69	1.63	0.83	0.18	0.09	2.48	2.43	1.31	0.37	0.27

### 3.6.3 As(V) and Cr(VI) adsorption isotherm models

Figure 6 reports the plot of  $Q_e$  versus  $C_e$  experimental data. The Langmuir equation reported in the experimental section was used to describe the adsorption isotherm model. By applying the non-linear curve-fit on the equation,  $R^2$  value of 0.974 and 0.992 were obtained for As(V) and Cr(VI), respectively. Thus, in both cases a monolayer sorption behaviour can be assumed, extrapolating as maximum sorption ability ( $Q_m$ ) 76.3 mg/g and 130.9 mg/g for As(V) and Cr(VI) respectively.

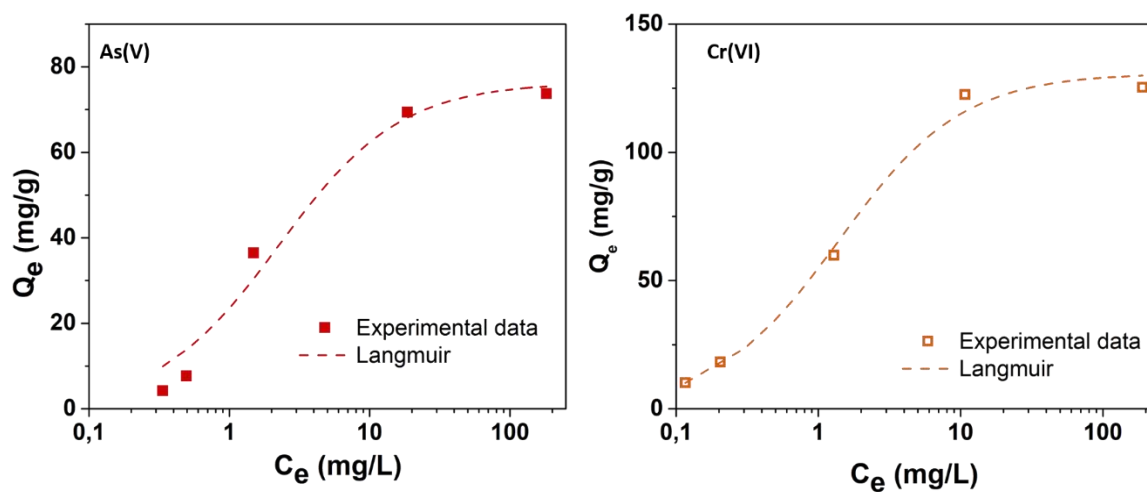


**Figure 6.** Equilibrium adsorption isotherms for As(V) on the left and Cr(VI) on the right for VbNMG-100 cryogel.

**Table 4** reports the  $Q_m$  values of VbNMG-100 and similar NMG-based polymers reported in literature [31,39,41,42]. Our cryogel exhibited pretty much better performance in terms of  $Q_m$  values if compared with the commercial IRA-743, NMG based resins [31,39,41] as well as other commercial products used to this purpose [41,42]. If compared with other polymeric systems formulated for As(V) and Cr(VI) removal VbNMG-100 cryogel can be placed in a competitive position [12,18,22,36,54-57].

**Table 4.** A comparison of  $Q_m$  values of NMG-based polymers reported in literature with the as-synthesized VbNMG-100 cryogel. All compared data are referred to batch equilibrium experiments tested at similar  $C_0$  and performed at pH=6.

Year	NMG-based material	As(V) $Q_m$ (mg g <sup>-1</sup> )	Cr(VI) $Q_m$ (mg g <sup>-1</sup> )	T(°C)	Time of contact	References
2020	VbNMG-100	76.34	130.85	RT	24h	This work
2019	MS-HZO	5.78	/	RT	24h	[31]
2012	PVbNMDG nanocomposite	55.24	/	RT	48h	[31,39]
2004	NMDG	60.5	/	RT	3d	[41]
2004	IRA 743	14.7	/	RT	3d	[41]
2010	IRA-743	/	29.35	RT	60 min	[42]

### 3.6.4 Interfering Tests

It is well known that oxyanions like sulphate and phosphate are commonly present in groundwater and wastewater at concentration higher than those of metal ions. Due to their charge as well as structural similarities with arseniate, sulphate and phosphate compete with the active sites of adsorbent materials during the sorption process [35,39]. Therefore, the interference of the aforementioned oxyanions was studied by increasing their concentration from 0 to 480 mg/L at a fixed As(V) concentration of 30 mg/L. The obtained results were reported in **Figure 7**.

It can be observed that the presence of phosphate did not disturb the sorption process of the cryogel for all oxyanion concentration tested, maintaining high sorption retention (~99%). Whereas, As(V) capture was affected by the presence of sulphate, indeed, by adding concentration higher than 60 mg/L, As(V) uptake reduction from 98% to 12,3% was observed.

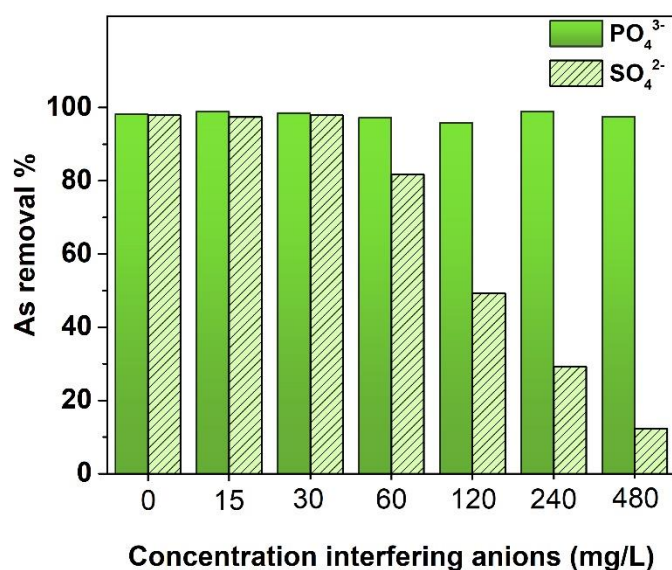


**Figure 7.** Effect of phosphate (green bar) and sulphate (green medium bar) oxyanions on As(V) adsorption [oxyanions dosage: 0-480 mg/L, As(V) solution: 7.7 mg/L].

### 3.6.5 Sorption-Desorption cycles

To evaluate the adsorbent lifetime, adsorption/desorption experiments were carried up to 6 subsequent cycles. Specifically, the VbNMG-100 cryo-sponge was swelled with As(V) solution, that was removed after 5 minutes of contact time. The quantified withdrawal of As(V) from the solution demonstrated a very fast adsorption process without any destruction of the sponge. In particular, **Figure 8 (b)** shows that VbNMG cryogel did not lose its capture efficiency, maintaining constant the As(V) uptake for all tested cycles.

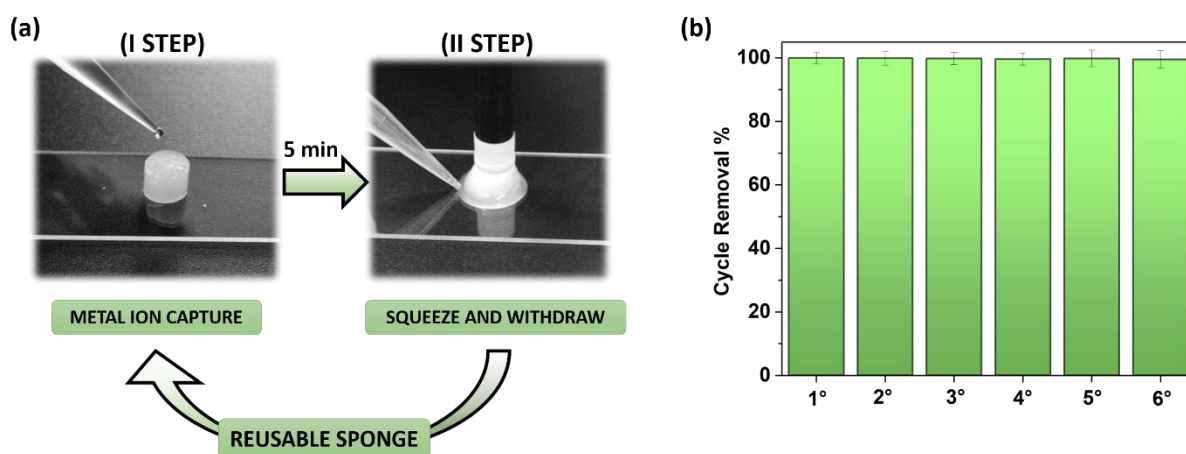
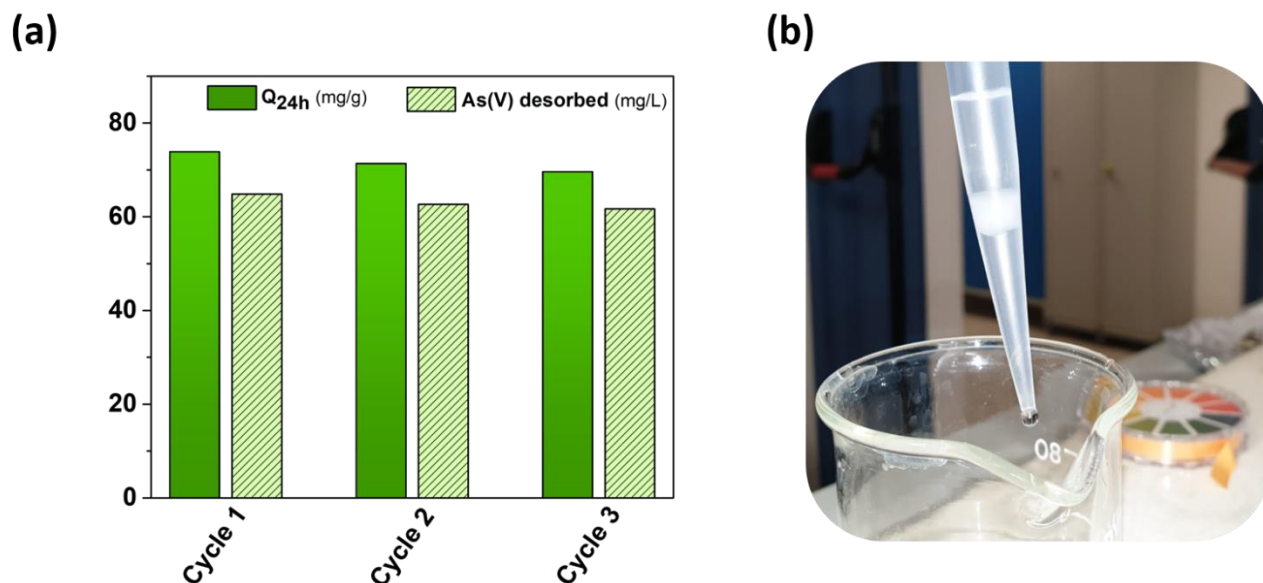


**Figure 8.** (a) Scheme of the purification process repeated up to 6 cycles. After 5 minutes of contact time the arsenate solution (30 mg/L) was removed by a simple cryogel squeezing. (b) ICP-MS of the withdrawn As(V) solutions showed a removal of ~99% up to 6 repeated cycles.

1 Based on these outstanding results, regeneration tests to verify the recyclability of VbNMG-100  
2 cryogel were carried out up to three cycles (see experimental section). From **Figure 9 (a)** it is possible  
3 to appreciate the high  $Q_e$  values obtained for all tested cycles as well as the ability of HCl solution in  
4 regenerating the sponge. Moreover, the effective removal of As(V), was further corroborated by  
5 calculating the As(V) residue in water after each cycle. Thus, it can be considered a further proof of  
6 the excellent performance of NMG cryogel in sorption/elution cycles.  
7  
8  
9  
10  
11  
12



15  
16  
17  
18  
19  
20  
21  
22  
23  
24  
25  
26  
27  
28  
29  
30  
31  
32  
33 **Figure 9.** Cryogel regeneration experiment ( $C_0=1400$  mg/L of arsenate salt,  $m_{\text{cryogel}}=20$  mg). **(a)** three  
34 subsequent cycles of As(V) adsorption (green bars) and desorption (green medium bars) after 24h of  
35 contact time. **(b)** The arranged system used to regenerate the sponge by HCl 1M (3 mL).  
36  
37  
38  
39

#### 40 **4. Conclusions**

41  
42 A novel approach to eliminate As(V) and Cr(VI) from water by using polymeric macroporous  
43 materials based on NMG was proposed. The sponges obtained by cryo-structuration in water, showed  
44 significant sequestrant activity versus both metal ions even using them in low amounts. Specifically,  
45 VbNMG-100 cryogel showed outstanding performance in removing metals ions from water with a  
46 fast sorption ability. This peculiar property is reasonably ascribed to the macroporous nature of  
47 cryogels that provides water fast-diffusion pathway, determining a boost in the metal ions chelation.  
48 Indeed, As(V) as well as Cr(VI) removal of VbNMG-100 offered pretty much superior values if  
49 compared to other similar NMG-based formulates. Furthermore, *via* a simple squeeze process, it is  
50 possible to withdraw purified water after only 5 min of contact time, obtaining the 99% of As(V) ion  
51 capture for each cycle. The sponges can be also reused up to 5 times without any significant loss of  
52  
53  
54  
55  
56  
57  
58  
59  
60  
61  
62  
63  
64  
65

1  
2 sequestration performance and their regeneration was achieved by a facile acid treatment up to three  
3 cycles, restoring the initial chelating properties.  
4  
5  
6

## 7 **References**

- 8  
9 [1] M. M. Mekonnen, A. Y. Hoekstra, Four billion people facing severe water scarcity *Sci. Adv.* 2  
10 (2016) e1500323;  
11  
12 [2] S. Bolisetty, M. Peydayesh, R. Mezzenga, Sustainable technologies for water purification from  
13 heavy metals: review and analysis, *Chem. Soc. Rev.*, 48 (2019) 463-487;  
14  
15 [3] P. B Tchounwou, C.t G Yedjou, A. K Patlolla, D. J Sutton, Heavy Metals Toxicity and the  
16 Environment, NIH Public Access 2012 ; 101: 133–164. doi:10.1007/978-3-7643-8340-4\_6;  
17  
18 [4] J. H. Duffus, "Heavy metals" a meaningless term?(IUPAC Technical Report), *Pure and applied*  
19 *chemistry*, 74(5) (2002) 793-807;  
20  
21 [5] H. Bradl, (Ed.), *Heavy metals in the environment: origin, interaction and remediation*, Elsevier,  
22 2005;  
23  
24 [6] D. K. Gupta, S. Tiwari, B.H.N. Razafindrabe, S. Chatterjee *Arsenic Contamination from*  
25 *Historical Aspects to the Present*, Springer International Publishing AG 2017 D.K. Gupta, S.  
26 Chatterjee (eds.), *Arsenic Contamination in the Environment*, DOI 10.1007/978-3-319-54356-  
27 7\_1  
28  
29 [7] *Drinking Water Parameter Cooperation Project: Support to the revision of Annex I Council*  
30 *Directive 98/83/EC on the Quality of Water Intended for Human Consumption (Drinking Water*  
31 *Directive)*, (2017) WHO: Geneva, Switzerland;  
32  
33 [8] S. Chowdhury, M. J. Mazumder, O. Al-Attas, T. Husain, Heavy metals in drinking water:  
34 occurrences, implications, and future needs in developing countries, *Sci. total Environ.*, 569  
35 (2016) 476-488;  
36  
37 [9] Y. Salameh, A. B. Albadarin, S. Allen, G. Walker, M.N.M. Ahmad, Arsenic (III, V) adsorption  
38 onto charred dolomite: charring optimization and batch studies, *Chem. Eng. J.*, 259 (2015) 663-  
39 671;  
40  
41 [10] C. F. Carolin, P. S. Kumar, A. Saravanan, G. J. Joshiba, M. Naushad, Efficient techniques for  
42 the removal of toxic heavy metals from aquatic environment: A review., *J. Environ. Chem. Eng.*,  
43 5(3) (2017) 2782-2799;  
44  
45 [11] Y. Huang, X. Feng, Polymer-enhanced ultrafiltration: Fundamentals, applications and recent  
46 developments, *J. Memb. Sci.*, 586 (2019) 53–83;  
47  
48  
49  
50  
51  
52  
53  
54  
55  
56  
57  
58  
59  
60  
61  
62  
63  
64  
65



- 1  
2  
3  
4  
5  
6  
7  
8  
9  
10  
11  
12  
13  
14  
15  
16  
17  
18  
19  
20  
21  
22  
23  
24  
25  
26  
27  
28  
29  
30  
31  
32  
33  
34  
35  
36  
37  
38  
39  
40  
41  
42  
43  
44  
45  
46  
47  
48  
49  
50  
51  
52  
53  
54  
55  
56  
57  
58  
59  
60  
61  
62  
63  
64  
65
- [12] Y. Deng, Q. Zhang, Q. Zhang, Y. Zhong, P. Peng, Arsenate removal from underground water by polystyrene-confined hydrated ferric oxide (HFO) nanoparticles: effect of humic acid, *Environ. Sci. Pollut. Res.*, 27 (2020) 6861–6871;
- [13] T. V. Nguyen, S. Vigneswaran, H. H. Ngo, J. Kandasamy, Arsenic removal by iron oxide coated sponge: Experimental performance and mathematical models, *J. Hazard. Mater.* 182 (2010) 723–729;
- [14] S. R. Chowdhury, E. K. Yanful, Arsenic and chromium removal by mixed magnetite-maghemite nanoparticles and the effect of phosphate on removal, *J. Environ. Manage.* 91 (2010) 2238–2247;
- [15] S. Pathan, S. Bose, Arsenic Removal Using “Green” Renewable Feedstock-Based Hydrogels: Current and Future Perspectives, *ACS Omega*, 3 (2018) 5910–5917;
- [16] S. Anjum, D. Gautam, B. Gupta, S. Ikram, Arsenic Removal from Water: An Overview of Recent Technologies, *The IUP Journal of Chemistry*, Vol. II, No. 3, 2009;
- [17] Q. Wu, M. Liu, X. Wang, A novel chitosan based adsorbent for boron separation, *Sep. Purif. Technol.* 211 (2019) 162–169;
- [18] F. Su, H. Zhou, Y. Zhang, G. Wang, Three-dimensional honeycomb-like structured zero-valent iron/chitosan composite foams for effective removal of inorganic arsenic in water, *J. Colloid Interfac. Sci.* 478 (2016) 421–429;
- [19] B. Moraga, L. Toledo, L. Jelínek, J. Yanez, B. L. Rivas, B. F. Urbano, Copolymer- hydrous zirconium oxide hybrid microspheres for arsenic sorption, *Water Res.* 166 (2019) 115044;
- [20] C. Balan, I. Volf, D. Bilba, Chromium (VI) Removal from Aqueous solutions by purolite base anion- exchange resins with gel, *Chem. Ind. Chem. Eng. Q.* 19 (4) (2013) 615–628;
- [21] A. Dąbrowski, Adsorption—from theory to practice. *Adv. Colloid Interfac.* 93(1-3) (2001) 135–224;
- [22] J. Jachuła, Z. Hubicki, Removal of Cr(VI) and As(V) ions from aqueous solutions by polyacrylate and polystyrene anion exchange resins, *Appl. Water Sci.* 3 (2013) 653–664;
- [23] I. Ali, V. K. Gupta, Advances in water treatment by adsorption technology. *Nat. Protoc.*, 1(6) (2006) 2661;
- [24] D.B. Singh, G. Prasad, D.C. Rupainwar, Adsorption technique for the treatment of As(V)-rich effluents, *Colloids Surfaces A: Physicochem. Eng. Aspects* 111 (1996) 49–56;
- [25] N. Ricci Nicomel, K. Leus, K. Folens, P. Van Der Voort, G. Du Laing, Review Technologies for Arsenic Removal from Water: Current Status and Future Perspectives, *Int. J. Environ. Res. Public Health* 13(2016) 62;
- [26] D. Mohana, C. U. Pittman Jr. Arsenic removal from water/wastewater using adsorbents—A critical review, *J. Hazard. Mater.* 142 (2007) 1–53;



- 1 [27] M. Ussia, A. Di Mauro, T. Mecca, F. Cunsolo, G. Nicotra, C. Spinella, P [10.1021/ie502512h](https://doi.org/10.1021/ie502512h).  
2 Cerruti, G. Impellizzeri, V. Privitera, S. C. Carroccio, ZnO–pHEMA Nanocomposites: An  
3 Ecofriendly and Reusable Material for Water Remediation. *ACS Appl. Mater. Inter.*, 10(46)  
4 (2018) 40100-40110;  
5  
6  
7 [28] H. Wang, X. Ji, M. Ahmed, F. Huang, J. L. Sessler, Hydrogels for anion removal from water, *J.*  
8 *Mater. Chem. A* 7 (2019) 1394;  
9  
10 [29] S. C. Tang, D. Y. Yan, I. M. Lo, Sustainable wastewater treatment using microsized magnetic  
11 hydrogel with magnetic separation technology, *Ind. Eng. Chem. Res.*, 53(40) (2014) 15718-  
12 15724;  
13  
14  
15 [30] S. Chatterjee, M. W. Lee, S. H. Woo, Adsorption of congo red by chitosan hydrogel beads  
16 impregnated with carbon nanotubes, *Bioresour. Technol.*, 101(6) (2010) 1800-1806;  
17  
18 [31] B. F. Urbano, B. L. Rivas, F. Martinez, S. D. Alexandratos, Water-insoluble polymer–clay  
19 nanocomposite ion exchange resin based on N-methyl-D-glucamine ligand groups for arsenic  
20 removal, *React. Funct. Polym.* 72 (2012) 642–649;  
21  
22  
23 [32] U. Schilde, H. Kraudelt, E. Uhlemann, Separation of the oxoanions of germanium, tin, arsenic,  
24 antimony, tellurium, molybdenum and tungsten with a special chelating resin containing  
25 methylaminoglucitol groups, *React. Polym.* 22 (1994) 101-106;  
26  
27  
28 [33] I. Polowczyk, P. Cyganowski, B. F. Urbano, B. L. Rivas, M. Bryjak, N. Kabay, Amberlite IRA-  
29 400 and IRA-743 chelating resins for the sorption and recovery of molybdenum(VI) and  
30 vanadium(V): Equilibrium and kinetic studies, *Hydrometallurgy* 169 (2017) 496–507;  
31  
32  
33 [34] G. Ozkula, B. F. Urbano, B. L. Rivas, N. Kabay, M. Bryjak, Arsenic Sorption using mixtures  
34 on ion exchange resins containing N- Methyl-Dglucamine and quaternary ammonium groups, *J.*  
35 *Chil. Chem. Soc.*, 61(1) (2016) 2752-2756;  
36  
37  
38 [35] I. Polowczyk, B. F. Urbano, B. L. Rivas, M. Bryjak, N. Kabay, Equilibrium and kinetic study of  
39 chromium sorption on resins with quaternary ammonium and N-methyl-D-glucamine groups,  
40 *Chem. Eng. J.* 284 (2016) 395–404;  
41  
42  
43 [36] B. L. Rivas, J. Sánchez, Soluble polymer containing an N-methyl-D-glucamine ligand for the  
44 removal of pollutant oxy-anions from water, *ACS In Stereochemistry and Global Connectivity:*  
45 *The Legacy of Ernest L. Eliel Volume 1* (pp. 197-211);  
46  
47  
48 [37] P. Santander, B. L. Rivas, B. Urbano, L. Leiton, I. Y. Ipek, M. Yuksel, N. Kabay, M. Bryjak,  
49 Removal of Cr(VI) by a chelating resin containing N-methyl-D-glucamine, *Polym. Bull.* 71  
50 (2014) 1813–1825;  
51  
52  
53  
54  
55  
56  
57  
58  
59  
60  
61  
62  
63  
64  
65

- 1  
2  
3  
4  
5  
6  
7  
8  
9  
10  
11  
12  
13  
14  
15  
16  
17  
18  
19  
20  
21  
22  
23  
24  
25  
26  
27  
28  
29  
30  
31  
32  
33  
34  
35  
36  
37  
38  
39  
40  
41  
42  
43  
44  
45  
46  
47  
48  
49  
50  
51  
52  
53  
54  
55  
56  
57  
58  
59  
60  
61  
62  
63  
64  
65
- [38] L. Toledo, B. L. Rivas, B. F. Urbano, J. Sánchez, Novel N-methyl-D-glucamine-based water-soluble polymer and its potential application in the removal of arsenic, *Sep. Purif. Technol.* 103 (2013) 1–7;
- [39] B. F. Urbano, B. L. Rivas, F. Martínez, S. D. Alexandratos, Equilibrium and kinetic study of arsenic sorption by water-insoluble nanocomposite resin of poly[N-(4-vinylbenzyl)-N-methyl-D-glucamine]-montmorillonite, *Chem. Eng. J.* 193–194 (2012) 21–30;
- [40] T. M. Ting, M. M. Nasef, K. Hashimb, Tuning N-methyl-D-glucamine density in a new radiation grafted poly(vinyl benzyl chloride)/nylon-6 fibrous boron-selective adsorbent using the response surface method, *RSC Adv.*, 5 (2015) 37869;
- [41] L. Dambies, R. Salinaro, S. D. Alexandratos, Immobilized N-Methyl-D-glucamine as an arsenate-selective resin, *Environ. Sci. Technol.* 38 (2004) 6139-6146;
- [42] M. R. Gandhi, N. Viswanathan, S. Meenakshia, Adsorption mechanism of hexavalent chromium removal using Amberlite IRA 743 resin, *Ion Exch. Lett.*, 3 (2010) 25-35;
- [43] S. Sayin, F. Ozcan, M. Yilmaz, Synthesis and evaluation of chromate and arsenate anions extraction ability of a N-methylglucamine derivative of calix[4]arene immobilized onto magnetic nanoparticles, *J. Hazard. Mater.* 178 (2010) 312–319;
- [44] M. M. Nasef, T.M. Ting A. Abbasi, A. Layeghi-moghaddam, S. S. Alinezhad, K. Hashim, Radiation grafted adsorbents for newly emerging environmental applications, *Radiat. Phys. Chem.* 118 (2016) 55–60;
- [45] D. C. Wang, H. Y. Yu, M. L. Song, R. T. Yang, J. M. Yao, Superfast adsorption–disinfection cryogels decorated with cellulose nanocrystal/zinc oxide nanorod clusters for water-purifying microdevices. *ACS Sustain. Chem. Eng.*, 5(8) (2017) 6776-6785;
- [46] O. Okay, (Ed.), *Polymeric Cryogels: Macroporous gels with remarkable properties* (2014) Vol. 263 Springer;
- [47] A. Bonilla-Petriciolet, D. I. Mendoza-Castillo, H. E. Reynel-Ávila, (Eds.) *Adsorption processes for water treatment and purification* (2017) Netherlands: Springer;
- [48] Y. S. Ho, Review of second-order models for adsorption systems. *Journal of hazardous materials*, 136(3) (2006) 681-689;
- [49] G. Alberti, V. Amendola, M. Pesavento, R. Biesuz, Beyond the synthesis of novel solid phases: review on modelling of sorption phenomena. *Coord. Chem. Rev.*, 256(1-2) (2012) 28-45;
- [50] T. M. Ting, M. M. Nasef, K. Hashim, Tuning N-methyl-D-glucamine density in a new radiation grafted poly (vinyl benzyl chloride)/nylon-6 fibrous boron-selective adsorbent using the response surface method. *RSC Advances*, 5(47) (2015) 37869-37880;

- 1 [51] D. Robati, Pseudo-second-order kinetic equations for modeling adsorption systems for removal  
2 of lead ions using multi-walled carbon nanotube. *J. Nanostructure Chem.*, 3(1) (2013) 55;
- 3 [52] C. Balan, I. Volf, D. Bilba, Chromium (VI) removal from aqueous solutions by purolite base  
4 anion-exchange resins with gel structure, *Chem. Ind. Chem. Eng. Q.*, 19(4) (2013) 615-628;
- 5 [53] J. A. R. Guivar, A. Bustamante, J. C. Gonzalez, E. A. Sanches, M. A. Morales, J. M. Raez, M. J.  
6 L. Muñoz, A. Arencibia, Adsorption of arsenite and arsenate on binary and ternary magnetic  
7 nanocomposites with high iron oxide content. *Applied Surface Science*, 454, (2018). 87-100;
- 8 [54] B. Moraga, L. Toledo, L. Jelínek, J. Yanez, B. L. Rivas, B. F. Urbano, Copolymer- hydrous  
9 zirconium oxide hybrid microspheres for arsenic sorption, *Water. Res.* 166 (2019) 115044;
- 10 [55] H. Bessaies, S. Iftekhhar, B. Doshi, J. Kheriji, M. C. Ncibi, V. Srivastava, M. Sillanpää, B.  
11 Hamrouni, Synthesis of novel adsorbent by intercalation of biopolymer in LDH for the removal  
12 of arsenic from synthetic and natural water, *J. Environ. Sci.*, 91 (2020) 246-261;
- 13 [56] J. S. Mankar, M. D. Sharma, R. J. Krupadam, Molecularly imprinted nanoparticles (nanoMIPs):  
14 an efficient new adsorbent for removal of arsenic from water, *J. Mater. Sci.*, (2020) 1-16;
- 15 [57] D. V. Morales, B.L. Rivas, N. Escalona, Poly([(2-methacryloyloxy)ethyl]trimethylammonium  
16 chloride): synthesis, characterization, and removal properties of As(V), *Polym. Bull.* 73 (2016)  
17 875–890;
- 18  
19  
20  
21  
22  
23  
24  
25  
26  
27  
28  
29  
30  
31  
32  
33  
34  
35  
36  
37  
38  
39  
40  
41  
42  
43  
44  
45  
46  
47  
48  
49  
50  
51  
52  
53  
54  
55  
56  
57  
58  
59  
60  
61  
62  
63  
64  
65



Click here to access/download  
**Supplementary Material**  
Supporting information.docx



**Declaration of interests**

The authors declare that they have no known competing financial interests or personal relationships that could have appeared to influence the work reported in this paper.

The authors declare the following financial interests/personal relationships which may be considered as potential competing interests: